

pH Control of Conductance in a Pyrazolyl Langmuir-Blodgett Monolayer

L. Herrer,^{a,b} S. Martín,^{a,b,c} A. González-Orive,^d D. C. Milan,^e A. Vezzoli,^e R. J. Nichols,^{e*}

J. L. Serrano,^{a,f*} and P. Cea.^{a,b,c*}

- ^[a] Instituto de Nanociencia y Materiales de Aragón (INMA), CSIC-Universidad de Zaragoza, Zaragoza 50009, Spain.
- ^[b] Departamento de Química Física, Facultad de Ciencias, Universidad de Zaragoza, 50009, Zaragoza, Spain.
- ^[c] Laboratorio de Microscopias Avanzadas (LMA). Universidad de Zaragoza, Edificio I+D+i. 50018, Zaragoza, Spain.
- ^[d] Department of Chemistry, Materials and Nanotechnology Institute, University of La Laguna, 38200, La Laguna, Tenerife, Canary Islands, Spain.
- ^[e] Department of Chemistry, University of Liverpool, Crown Street, Liverpool, L69 7ZD, United Kingdom.
- ^[f] Departamento de Química Orgánica, Facultad de Ciencias, Universidad de Zaragoza, 50009, Zaragoza, Spain.

Abstract

In this contribution, pyrazole is identified as an excellent anchoring group capable to form well-ordered Langmuir-Blodgett (LB) monolayers onto gold substrates. In contrast, formation of self-assembled (SA) monolayers is prevented due the extraction of gold atoms from the surface upon the incubation process required for the formation of these films. The electronic coupling strength of pyrazole-gold junctions is explored through evaluation of the electrical properties of LB films incorporating a double pyrazole terminated molecular wire, namely 1,4-bis(1H-pyrazol-4-ylethynyl)benzene, **1**; these electrical properties are compared with those of molecules having a similar chemical structure, geometry and length. The conductance value for LB films of **1** is high when the monolayer is transferred from a Langmuir film prepared onto a basic subphase, $1.19 \cdot 10^{-4} G_0$, as it is more than four times larger than the conductance of the same compound incorporated on a LB film prepared from a water subphase, $0.27 \cdot 10^{-4} G_0$. These results are interpreted in terms of the deprotonation of the pyrazole group in a basic media that leads to formation of the pyrazolate (deprotonated pyrazole) moiety. This results in a more efficient electronic coupling with the gold tip of the scanning tunnelling microscope used for the film characterization.

Introduction

Molecular electronics strives not only towards the eventual use of molecules as functional elements for circuitry, but also towards their use in applications as diverse as energy (e.g. solar-energy harvesting, thermoelectric devices), nanochemistry (catalysis, single molecule reactions), and optoelectronics (single molecule OLEDs, use of illumination to control transport through the junction).¹⁻⁶ In molecular electronics, the chemical structure of the molecule, the nature of the electrode and the surface chemistry operating between the molecule and the electrode are key factors, which can determine device functionality, reproducibility, processability, scalability, and yield in large area devices.⁷⁻⁹ Here the anchor group is recognized as a crucial element in the design of molecular devices. Recently, attention has been paid to multidentate anchoring groups that could provide enhanced chemical and “mechanical” stability as well as improved electronic coupling. By contrast, fluxional bonds are best avoided in which there is a dynamic formation and rupture of bonds between the molecule and the metal atoms of the surface (e.g. the gold-sulfur contact which is one reason behind the observed conductance fluctuations in thiol-gold junctions). Ideally one wants to avoid such dynamic formation and rupture of bonds between the anchor group and the metal atoms on the surface. Examples of multidentate anchoring groups include bidentate moieties such as dithiols,¹⁰⁻¹¹ norbornyldithiol,¹² carboxylic acids,¹³⁻¹⁴ dithiocarbamates,¹⁵ carbodithiolates,¹⁶ dithiocarboxylic acids,¹⁶ tetrathialfulvalenes,¹⁷⁻¹⁸ phosphonic acids,¹⁹⁻²⁰ pyrazole,²¹ 2-aminepyridine,²² and catechols.²³ Multipodal platforms (i.e. molecules having several anchoring units) have also been explored under the same premises.²⁴⁻³² Many of these studies employing multidentate molecules have been done at the single molecule level, but their assembly in large area devices and the determination of their ensemble electrical properties is a current topic of interest.

Pyrazole is a 5-membered heteroaromatic ring incorporating two adjacent nitrogen atoms. In contrast with other heteroaromatic rings such as imidazole, the contiguous location of the two potential anchoring nitrogen atoms (pyridine-like and pyrrole-like nitrogens) of the pyrazole ring results in a prospective bidentate ligand. This facilitates the coordination to metallic centers situated at a short distance and makes this moiety particularly interesting as a surface binding group in molecular electronics. Additionally, the pyrazole moiety can act as a moderately weak acid (pyrrole-type nitrogen atom with proton-donor behaviour). Recently, we reported the unconventional single molecule

conductance behaviour of a pyrazole-terminated molecular wire, 1,4-bis(1H-pyrazol-4-ylethynyl)benzene, Figure 1, hereafter denoted as **1**.²¹ The pyrazole group attached to the bottom electrode was chemisorbed through a deprotonation process, whilst the opposite pyrazole group in contact with the scanning tunnelling microscope (STM) tip changed its protonation state and contact binding geometry during junction evolution. This resulted in a sharp increase in conductance during the retraction of the STM tip and junction stretching, as a result of a deprotonation.²¹

The influence of the pH on the molecular conductance of metal-molecule junctions has been analysed only in a relatively few studies. Li et al.³³ studied the conductance of two dyes, malachite green and pararosaniline when the surrounding pH changed, constructing a switch predicated on pH actuating changes in the conjugation and electronic structure of the molecules. Dual control of molecular conductance under both an acid media and visible-light irradiation through a photoinduced proton-transfer (PIPT) strategy was also demonstrated.³⁴ In another study of pH effects on molecular junctions, Brooke et al. modulated the conductance of 4,4'-vinylenedipyridine (44VDP) molecular junctions with Ni contacts both by the applied electrochemical gate voltage and by the pH of the solution.³⁵ They observed that the Ni|44VDP|Ni junction can operate as a pH-sensitive switch where the pH value at which conductance switching takes place could be electrically tuned. In addition, they reported the observation of proton transfer to and from a single molecule. On the other hand, conductance in large area molecular electronic devices could also be tuned by pH. Monolayers featuring carboxylic groups exhibited lateral intermolecular H-bonding, and these lateral interactions could be broken by deprotonation in a basic media which leads to H-bond cleavage and conductance enhancement in basic media.¹⁴ Electron transfer in molecules interacting through non-covalent interactions has also attracted interest under the premise that the molecular conductance can be switched ON and OFF by changing the solution pH.³⁶ Wu et al.³⁷ have demonstrated the formation of oligomeric chains of imidazole due to hydrogen bonding networks, promoted by the pH of the media, that resulted in efficient charge transport. Hydrogen bonding dynamics has also been studied using DNA base pairs, where H-bonding across molecular junctions was achieved.³⁸⁻³⁹ Pan et al.⁴⁰ have described the role of pH in a mechanism for the creation of single molecule-metal junctions through a robust imidazolate-gold chemisorption. Recently, Ai et al.⁴¹ have studied the electrical properties of molecular junctions formed with pH-responsive supramolecular systems. They showed that the conductance of

cucurbit[7]uril (host) and melphalan (guest) supramolecular complexes decreased as the pH increased.

The studies highlighted in the preceding paragraph collectively show that pH can be a valuable parameter in controlling molecular junctions. In this contribution, we explore how pH can be used to manipulate the electrical properties of compound **1**, which is a double pyrazole terminated molecular wire. We have previously demonstrated that the pyrazole terminal groups of **1** can be used to anchor molecular wires in between gold contacts. We extend our previous work with compound **1** in three ways by demonstrating:

- (i) The straightforward construction of large area devices by the Langmuir-Blodgett (LB) technique. By using the LB method it is possible to avoid the extraction of gold atoms from the surface observed in the self-assembly (SA) method which is a consequence of the strength of the pyrazolyl-gold junctions (~ 2 eV).²¹
- (ii) pH dependence of the conductance in monolayers of **1**, i.e., by a pH change in the preparation of the Langmuir films, where the pyrazole or pyrazolate terminal groups result in monolayers with a different electrical response (Figure 1).
- (iii) Pyrazole forms robust molecular junctions with improved electronic coupling in large area devices.

Experimental

Compound **1** was synthesized as previously described.^{21, 42} ¹H-NMR (400 MHz, DMSO-d₆, δ (ppm)): 7.95 (s, 4H), 7.47 (s, 4H), 6.14 (b, 2H). ¹³C-NMR (100 MHz, DMSO-d₆, δ (ppm)): 136.6, 131.2, 122.5, 100.8, 89.2, 84.0. NMR spectra were recorded on a Bruker AV-400 (operating at 400 MHz for ¹H and 100 MHz for ¹³C). These NMR spectra are available in the Supporting Information (SI), section 1. Elemental Analysis (EA) experimental (theoretical): %C 74.18 (74.40), %H 3.71 (3.91), %N 21.32 (21.69), performed in a Perkin-Elmer 2400, II microanalyser. MS: MALDI-TOF m/z: 258 (M⁺), performed using an ESI Bruker Esquire 300+, a MALDI+/TOF Bruker Microflex system. UV-vis spectra were recorded in a Varian Cary 50 Bio spectrophotometer.

Langmuir films and Langmuir-Blodgett (LB) monolayers were fabricated in a NIMA 702 BAM and KSV Nima KN 2003 troughs with dimensions 720 x 100 mm² and 580 x 145 mm², respectively, located at constant 20 °C in a clean room. A 2.5·10⁻⁵ M spreading solution of **1** was freshly prepared in a solvent mixture of THF:CHCl₃ (1:4 v/v) prior to each experiment. The subphases used were: pure water (Millipore Milli-Q, 18.2

M Ω ·cm, pH = 5.6, i.e. slightly acid due to the solubility of the CO₂ in the air and formation of H₂CO₃) and aqueous NaOH solution (pH = 11.0). Experimental conditions for the LB monolayers fabrication were: spread volume = 3 mL, 30 minutes for solvent evaporation, initial area per molecule = 1.5 nm²·molecule⁻¹, compression barrier speed = 6 mm·min⁻¹, transference onto the solid support at 10 mN·m⁻¹ (vertical dipping) and dipping speed = 2 mm·min⁻¹. Gold on glass substrates (from Arrandee™) were cleaned and flame annealed prior the transference of the Langmuir film. All samples were dried under a nitrogen stream.

X-ray photoelectron spectroscopy (XPS) was performed in a Kratos AXIS ultraDLD spectrophotometer including a monochromatic Al K α X-ray source (1486.6 eV) and a pass energy of 20 eV. XPS binding energies are referenced to the C1s peak at 284.6 eV. Atomic Force Microscopy (AFM) images were registered in tapping mode using a Bruker Nanoscope V operating in ambient conditions in air. RTESPA-150 AFM probes from Bruker (90-210 kHz, and 1.5 - 10 N·m⁻¹, nominal radius of 8 nm) were used. Images treatment and further analysis were performed on the Nanoscope off-line with software v.1.40.

The electrical characterization of compound **1** within the LB monolayers was carried out by using a Keysight Technology 5500 scanning tunneling microscope (STM) microscope and controller with Picoscan 5.3.3 software, operating in air. Current (I) – distance (s), or $I(s)$ calibration curves and $I-V$ curves were recorded on different but identically prepared samples. This included recording such measurements across different areas of the same sample to ensure a reproducible behaviour (see SI, section 6). STM tips were prepared by electrochemically etching of commercial Au wires (99.99%, 0.25 mm diameter, Goodfellow) in a 1:1 solution of HCl:EtOH at approximately +7.0 V.

Results

The self-assembly (SA) and the Langmuir-Blodgett (LB) techniques have been widely used for the fabrication of monolayers to build up large area devices in molecular electronics.⁴³ In the SA technique, the molecule is first adsorbed to the substrate and full ordering of the molecule comes later as adsorption progresses, while in the LB method the compound is first organized in a Langmuir film at the air-water interface and this pre-ordered film is subsequently transferred onto a solid substrate. However, in the case of compound **1**, standard self-assembly leads to gold surface etching enabling the formation

of gold-pyrazolate complexes in solution which can be analytically detected (see SI, section 3 for further details); therefore, the extraction of gold atoms from the bottom gold electrode upon the SA process prevents **1** from forming well-ordered monolayers by this methodology. In these circumstances, the Langmuir-Blodgett method is a powerful technique for the fabrication of high quality monolayers of compound **1** as demonstrated below.

Langmuir films of **1** were prepared as described in the experimental section using two different subphases, namely pure water (pH=5.6) and a basic aqueous solution of NaOH (pH=11.0). Figure 1 shows the different behaviour of the surface pressure vs. area per molecule isotherms of **1** in these two subphases. Both the area at which the take-off takes place and the area per molecule at a certain surface pressure are larger for the isotherm recorded onto a basic subphase. This result is interpreted in terms of a deprotonation of the pyrazole group in a basic pH, resulting in an ionized monolayer in which the electrostatic repulsion between neighbour molecules results in a larger area per molecule.⁴⁴ Furthermore, the deprotonation of the pyrazole group in compound **1** when it is exposed to a basic media was confirmed by ¹H-NMR experiments (see SI, section 2). Additionally, the surface potential vs. area per molecule isotherms were also recorded (Figure S6 in the SI), with these isotherms exhibiting a quite different behaviour for the monolayers formed either on a pure water or a NaOH aqueous solution. This result is also consistent with the deprotonation of **1** in contact with a basic subphase, which results in the formation of a negatively charged monolayer.

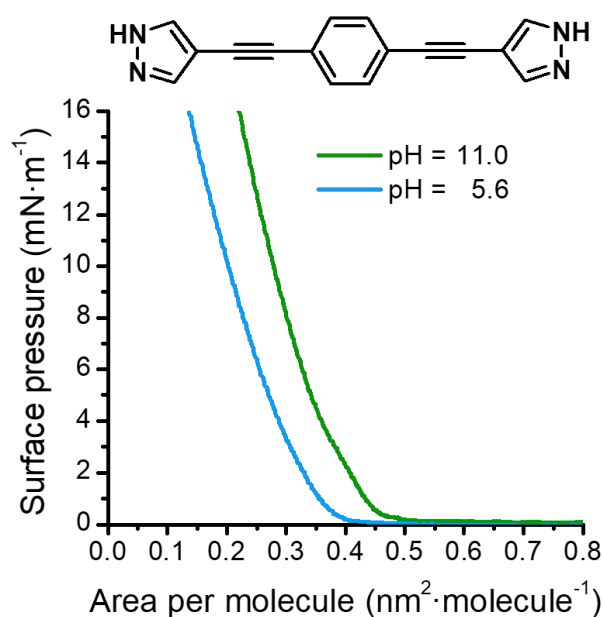


Figure 1. Molecular structure of 1,4-bis(1H-pyrazol-4-ylethynyl)benzene (**1**) and surface pressure vs. area per molecule for **1** recorded at 20 °C onto aqueous subphases at the indicated pH.

Atomic force microscopy (AFM) images of monolayer LB films of **1** transferred at $10 \text{ mN}\cdot\text{m}^{-1}$ from either a pH = 5.6 or pH = 11 subphase (Figure 2.b) show that homogeneous films are obtained (Figure S7 in the SI). The electrical properties of these LB films have been determined by using the so-called STM “Touch-To-Contact” method, abbreviated as the TTC method (see SI, section 6, for further details).⁴⁵⁻⁴⁷ In order to apply the TTC method, the thickness of the monolayer needs to be known in advance. In this case, the thicknesses of both LB films transferred from a water and a basic aqueous subphases were determined using the AFM tip lithography method, in which the tip is used to scratch the monolayer and determine its thickness, as described in the SI (Section 5). Accordingly, obtained thicknesses were $1.4 \pm 0.1 \text{ nm}$ and $1.6 \pm 0.1 \text{ nm}$ for the LB films prepared onto a water subphase and onto a basic subphase, respectively. Since the length of the molecule is 1.6 nm (as determined using Spartan[®] 14), compound **1** has a tilt angle of ca. 29° measured to the surface normal in LB films suspended on pure water, while it is oriented vertically with respect to the substrate in films formed on top of a basic subphase.

I-V curves of the monolayer LB films were recorded by the TTC method. In this method the STM tip just touches the monolayer and under such conditions single molecule contacts prevail, as shown by correspondence between values of TTC conductance and other single molecule methods for comparable molecular targets. In order to locate the STM tip just above the LB film, a calibration to determine the initial tip–substrate distance (s_0) was carried out. For this, 20 current-distance ($I(s)$) curves were recorded at different substrate locations for each LB monolayer at $I_0 = 10 \text{ nA}$ and $U_t = 0.6 \text{ V}$. Under these parameters, the STM tip is located within the LB film for both samples according to Equation 1 and the thicknesses of the monolayers (see Figure S7). Curves selected for this analysis showed a simple exponential decay of the tunnelling current indicating that molecules were not bridging between the substrate and the STM tip (see Figure S8 in SI). Using these current-distance curves, the current decay ($d \ln I / ds$) within the monolayer of **1** was determined by plotting $\ln I$ versus distance, s . Slopes of $7.2 \pm 1.2 \text{ nm}^{-1}$ and $5.6 \pm 0.8 \text{ nm}^{-1}$ for films prepared at pH=5.6 and 11 respectively, were obtained. These decay values are in good agreement with values obtained for comparable conjugated compounds.^{22, 48-49} Hence, by modifying the set-point current (I_0) and maintaining the tip bias (U_t) it is possible

to pinpoint the STM probe touching the top of the LB monolayer film by using Equation 1.

$$S = \frac{\ln(G_0 \times \frac{U_t}{I_0})}{d \ln(I) / ds} \quad (1)$$

where $G_0 = 2e^2/h$ is the quantum of conductance, $77.5 \mu\text{S}$.

Then, current–voltage (I – V) curves were recorded with the gold STM probe just in contact with the upper surface of the molecular monolayer film. Electrical characterisation entailed recording more than 400 I – V curves of **1** in monolayers prepared from both subphases, at pH=5.6 and pH=11. These curves were recorded from different regions of each sample, and from different samples prepared under the same experimental conditions to ensure reproducibility of the obtained results. Figure 2.b (right) shows the average I – V curves for each of the systems studied here. Conductance values were determined from the linear region in the average I – V curves (± 0.3 V). The electrical response of these two monolayers is very different, with conductance values of $0.27 \cdot 10^{-4} G_0$ (pH=5.6) and $1.19 \cdot 10^{-4} G_0$ (pH=11), respectively. This means that the monolayer of **1** prepared in basic conditions shows a conductance value more than 4 times larger than the conductance of the LB film prepared in pure water. The different conductance of these two monolayers of **1** prepared at different pH values in the Langmuir trough is attributed to the deprotonated pyrazolyl moieties arising from preparation with a basic subphase. The sodium pyrazolate at the STM tip-molecule contact results in more efficient electronic coupling and greater conductance (Figure 2.c).

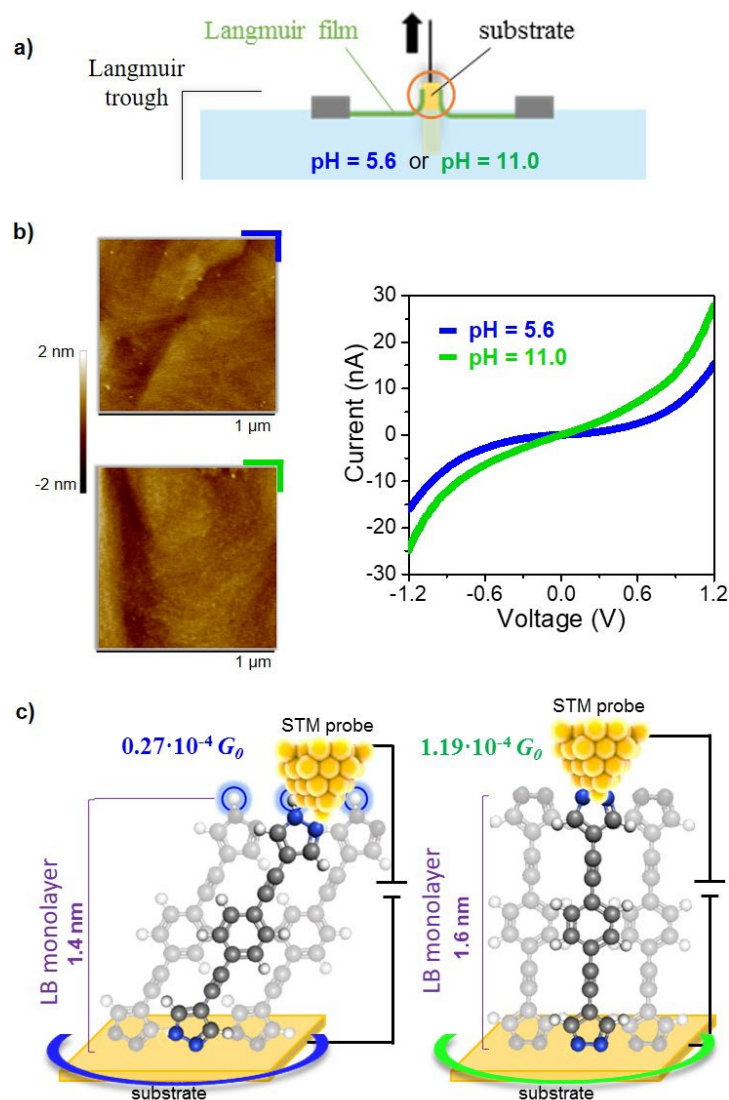


Figure 2. a) General scheme for the fabrication of the LB monolayers. b) Left panel: AFM images of LB monolayers as transferred from a pure water subphase (blue colored corner) and from a basic subphase (green colored corner). Right panel: averaged $I-V$ curves (from 421 and 481 $I-V$ traces at pH=5.6 and pH=11, respectively) recorded using the TTC method for LB films of **1** LBMs onto a pure water subphase, pH=5.6 (blue line) and onto a basic aqueous subphase, pH=11.0, (green line). c) Cartoon indicative of the chemical structure, orientation and conductance values obtained for LB monolayers of **1** transferred from aqueous subphases at pH = 5.6 (left) and pH = 11 (right).

In our previous contribution reporting the electrical behaviour of compound **1** in single molecule studies two conductance values, namely $3.4 \cdot 10^{-4} G_0$ and $2.3 \cdot 10^{-4} G_0$ were obtained with current versus junction-stretching distance curves exhibiting a peak-shape event just before junction rupture, instead of the more commonly observed plateau-like features. This unconventional result was explained, in terms of the chemical nature of the

heterocyclic pyrazole ring, which can be either protonated or deprotonated in the junction depending on the molecule-tip geometry.²¹ It was shown that the binding geometry and the low-to-high conductance transition can occur as the molecular junction is stretched as the STM tip is retracted. This model was supported by computations of the junction conductance for different surface anchoring. In this contribution in which we describe the properties of compound **1** incorporated in a monolayer, interpretation of the electrical properties must consider the molecule not as a single entity but (i) surrounded by neighbour molecules and (ii) located in a fix position with a predetermined geometry and orientation. The larger tilt of compound **1** with respect to the normal to the surface in a monolayer prepared in a subphase of pH=5.6 in comparison with pH=11 (as illustrated in Figure 2.c) might be expected to result in a larger conductance (the top and bottom electrodes are closer)⁵⁰ in the absence of other factors. This would be the likely expectation since more highly tilted conjugated molecular wires might generally be expected to couple more strongly to their electrode contact.⁵⁰⁻⁵¹ Nevertheless, the contrary effect is experimentally observed here, i.e. the less tilted monolayer gives a higher conductance. This result indicates that other factors determine the electrical behaviour of these monolayers. As it occurs in the case of bis-COOH OPE derivatives¹⁴ (see Table I), deprotonation processes prevent H-bonding intermolecular interactions between neighbouring molecules of compound **1** assembled in films. This fact has two effects, the first one is an increase of the area per molecule in the LB films (probably due to the electrostatic repulsion of the negatively charged molecules) and, secondly, it induces a perpendicular arrangement of **1** facing the gold substrate. Both facts determine the architecture of the molecules within the monolayer, which could be also responsible for a more efficient coupling of the molecule with the bottom electrode, contributing to the higher values of the conductivity observed in the deprotonated LB sample.

A model for the conductance values discussed is further explored by examining the surface adsorption properties of the molecular layers formed by the LB technique using different subphase pH values. The XPS spectra of LB films of compound **1** prepared onto subphases of pH= 5.6 and 11, together with the XPS spectrum of the powder of compound **1** were reported before in a contribution in which we studied the single molecule conductance of compound **1**.²¹ In this study we demonstrated that when compound **1** is transferred from a pure water subphase the pyrazole group in contact with the gold substrate is deprotonated as expected for a chemisorbed film. However, the external pyrazole group

remains protonated. In contrast, when compound **1** is transferred from a basic water subphase the two pyrazole groups in the molecule are deprotonated (see cartoon in Figure 2.c). The pyrazolate terminal group bears a negative charge – distributed between the two N atoms – which also enhances the binding ability of the pyrazolate group to the gold tip of the STM.

To further confirm the results provided by the XPS, the UV-vis spectra of LB films incorporating compound **1** from a pH=5.6 and pH=11 were recorded. Figure 3 show a UV-vis maximum absorption wavelength at 313 nm for LB films prepared onto a subphase of pH=5.6, which is shifted to 324 nm in films prepared in a pH=11 subphase. A shift in the UV-vis spectrum of compound **1** in solution towards larger wavelengths is observed after the addition of some drops of an aqueous solution of NaOH (from 315 nm to 334 nm). Such a bathochromic shift has been observed before⁵²⁻⁵³ for other pyrazole derivatives after deprotonation. Additionally, it is well-known that the pyrazole group has a large tendency to form NH...N intermolecular hydrogen bonds.⁵⁴⁻⁵⁶ Taken together, these results indicate that when the terminal group is in its pyrazole form (i.e. protonated) a less effective coupling of the molecule to the top-electrode (STM tip) results when compared with the direct strong chemical interaction between the ionized terminal pyrazolate group and the Au STM probe. Here it is also noted that when the top of the LB monolayer consists of the un-deprotonated pyrazole groups, these groups could associate through intermolecular hydrogen bonding. Such hydrogen bonding between neighbouring molecules in the pyrazole terminated LB films transferred from a water subphase could also lead to a less strong interaction with the STM tip as compared to a pyrazolate terminated LB film. This weaker interaction is attributable to the partial donation of electrons from the N atom of one molecule (pyridine-like nitrogen) to the H of the other molecule (H bonded to the nitrogen-like pyrrol) to form such H-bonds.

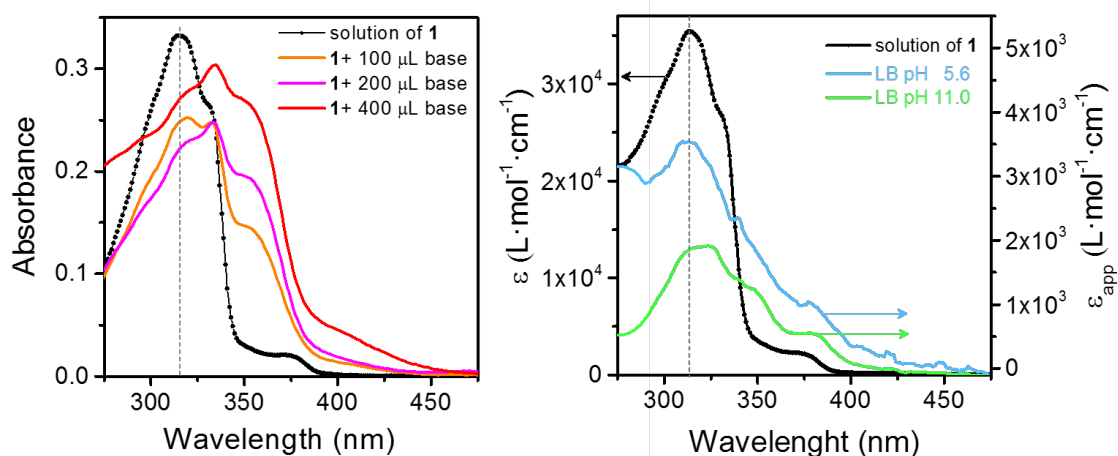
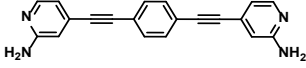
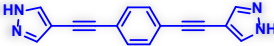


Figure 3. Left panel: UV-vis spectra of compound **1** in solution: (black) 10^{-5} M in THF:CHCl₃ 1:4; (orange) after addition of 100 μ L NaOH 5% (aq.); (magenta) after addition of 200 μ L NaOH 5% (ac.); (red) after addition of 400 μ L NaOH 5% (aq.). Right panel: (black) molar absorptivity for compound **1** in a THF:CHCl₃ 1:4 solution; (blue) apparent molar absorptivity for compound **1** in an LB film prepared from a water subphase, pH=5.6; (green) apparent molar absorptivity for compound **1** in an LB film prepared from a NaOH aqueous subphase, pH=11.0.

The conductance value for the LB of compound **1** fabricated in basic conditions is remarkably higher than those of molecules with similar structures (molecular wires with 3 aromatic rings) incorporated in monolayers assembled by the LB technique and characterized by the TTC method (Table I). This result further confirms an efficient electronic coupling between the pyrazole double anchoring group and gold.

Table I. Comparison of conductance values for monolayers incorporating the indicated molecular wires as determined by the TTC method.

Molecular Structure	Conductance (G ₀)	Monolayer thickness (nm)	Reference
	$0.26 \cdot 10^{-5}$ (pH=5.6) $1.75 \cdot 10^{-5}$ (pH=11.4)	1.81 ± 0.05 1.95 ± 0.05	14
	$1.20 \cdot 10^{-5}$	1.49 ± 0.04	57
	$1.37 \cdot 10^{-5}$	1.77 ± 0.05	49
	$3.90 \cdot 10^{-5}$	2.02 ± 0.05	46
	$5.17 \cdot 10^{-5}$	1.70 ± 0.05	48

	$6.20 \cdot 10^{-5}$	1.6 ± 0.1	22
	$2.7 \cdot 10^{-5}$ (pH=5.6) $11.9 \cdot 10^{-5}$ (pH=11.0)	1.4 ± 0.1 1.6 ± 0.1	This contribution

Conclusions

In this contribution the difficulties encountered with the preparation of conventional self-assembled monolayers of a molecule with terminal pyrazole groups have been discussed. The poor self-assembly is attributed to extraction of gold atoms from the surface. In contrast, homogeneous LB monolayers of 1,4-bis(1H-pyrazol-4-ylethynyl)benzene can be fabricated and this is demonstrated for two different pH subphases. Electrical characterization of these LB films was achieved with the STM probe touching against the top of the monolayer. Monolayers prepared by the LB method with a pure water (neutral pH) subphase displayed significantly different structural and electrical behavior compared to those prepared with an alkaline subphase. A stronger electronic coupling between the gold STM tip and the terminal pyrazolate group in comparison with the pyrazole results in conductance values of $1.19 \cdot 10^{-4} G_0$ (pH=11) and $0.27 \cdot 10^{-4} G_0$ (pH=5.6), respectively. Importantly, these values are the comparatively largest conductance values recorded using the touch to contact (TTC) STM method for ordered LB monolayers of comparable compounds in terms of length and chemical structure. This result further demonstrates that pyrazole is a promising bidentate terminal group for the assembly of large area molecular electronic devices.

Acknowledgements

This project was supported by the Spanish Ministry of Science through the grant numbers MAT2016-78257-R and PID2019-105881RB-I00, including FEDER funding, by Gobierno de Aragón through the grant numbers LMP33-18, and E31_20R with European Social Fund (Construyendo Europa desde Aragón). A.V. acknowledges funding from the Royal Society (URF\R1\191241).

References

1. Editorial, Does molecular electronics compute? *Nat. Nanotechnology* 2013, **8**, 377-377.
2. Editorial, Visions for a molecular future. *Nat. Nanotechnol.* 2013, **8**, 385-389.

3. Reece, G.; Scheurer, F.; Speisser, V.; Dappe, Y. J.; Mathevet, F.; Schull, G., Electroluminescence of a Polythiophene Molecular Wire Suspended between a Metallic Surface and the Tip of a Scanning Tunneling Microscope. *Phys. Rev. Lett.* 2014, **112**, 047403.
4. Xin, N.; Guo, X., Catalyst: The Renaissance of Molecular Electronics. *Chem. Asian J.* 2017, 373-376.
5. Hsu, L. Y.; Jin, B. Y.; Chen, C.-H.; Peng, S. M., Reaction: New Insights into Molecular Electronics. *Chem.* 2017, 378-379.
6. Ciampi, S.; Darwish, N.; Aitken, H. M.; Díez-Pérez, I.; Coote, M. L., Harnessing electrostatic catalysis in single molecule, electrochemical and chemical systems: a rapidly growing experimental tool box. *Chem. Soc. Rev.* 2018, **47**, 5146-5164.
7. Leary, E.; La Rosa, A.; Gonzalez, M. T.; Rubio-Bollinger, G.; Agrait, N.; Martín, N., Incorporating single molecules into electrical circuits. The role of the chemical anchoring group. *Chem. Soc. Rev.* 2015, **44**, 920.
8. Xin, N.; Guan, J.; Zhou, C.; Chen, X.; Gu, C.; Li, Y.; Ratner, M. A.; Nitzan, A.; Stoddart, J. F.; Guo, X., Concepts in the design and engineering of single-molecule electronic devices. *Nat. Rev. Phys.* 2019, **1**, 211-230.
9. Jia, C.; Guo, X., Molecule-electrode interfaces in molecular electronic devices. *Chem. Soc. Rev.* 2013, **42**, 5642-5660.
10. Casalini, S.; Berto, M.; Leonardi, F.; Operamolla, A.; Bortolotti, C. A.; Borsari, M.; Sun, W.; Felice, R. D.; Corni, S.; Albonetti, C.; Omar, O. H.; Farinola, G. M.; Biscarini, F., Self-Assembly of Mono- And Bidentate Oligoarylene Thiols onto Polycrystalline Au. *Langmuir* 2013, **29**, 13198-13208.
11. Rittikulsittichai, S.; Park, C. S.; Jamison, A. C.; Rodriguez, D.; Zenasni, O.; Lee, T. R., Bidentate Aromatic Thiols on Gold: New Insight Regarding the Influence of Branching on the Structure, Packing, Wetting, and Stability of Self-Assembled Monolayers on Gold Surfaces. *Langmuir* 2017, **33**, 4396-4406.
12. Darwish, N.; I., D.-P.; Da Silva, P.; Tao, N.; Gooding, J. J.; Paddon-Row, M. N., Observation of Electrochemically Controlled Quantum Interference in a Single Anthraquinone-Based Norbornylogous Bridge Molecule. *Angew. Chem. Int. Ed.* 2012, **51**, 3203-3206.
13. Camacho-Alanis, F.; Wu, L.; Zangari, G.; Swami, N., Molecular junctions of ~1 nm device length on self-assembled monolayer modified n- vs. p-GaAs. *J. Mater. Chem.* 2008, **18**, 5459-5467.
14. Ballesteros, L. M.; Martin, S.; Cortes, J.; Marques-Gonzalez, S.; Higgins, S. J.; Nichols, R. J.; Low, P. J.; Cea, P., Controlling the Structural and Electrical Properties of Diacid Oligo(Phenylene Ethynylene) Langmuir-Blodgett Films. *Chem. Eur. J.* 2013, **19**, 5352-5363.
15. von Wrochem, F.; Gao, D.; Scholz, F.; Nothofer, H.-G.; Nelles, G.; Wessels, J. M., Efficient electronic coupling and improved stability with dithiocarbamate-based molecular junctions. *Nat. Nanotechnol.* 2010, **5**, 618-624.
16. Denayer, J.; Delhalle, J.; Mekhalif, Z., Comparative study of copper surface treatment with self-assembled monolayers of aliphatic thiol, dithiol and dithiocarboxylic acid. *J. Electroanal. Chem.* 2009, **637**, 43-49.
17. Ditzler, L. R.; Karunatilaka, C.; Donuru, V. R.; Liu, H. Y.; Tivanski, A. V., Electromechanical Properties of Self-Assembled Monolayers of Tetrathiafulvalene Derivatives Studied by Conducting Probe Atomic Force Microscopy. *J. Phys. Chem. C.* 2010, **114**, 4429-4435.
18. Jayamurugan, G.; Gowri, V.; Hernández, D.; Martín, S.; González-Orive, A.; Dengiz, C.; Dumele, O.; Pérez-Murano, F.; Gisselbrecht, J.-P.; Boudon, C.; Schweizer, W. B.;

- Breiten, B.; Finke, A. D.; Jeschke, G.; Bernet, B.; Ruhlmann, L.; Cea, P.; Diederich, F., Design and synthesis of Aviram–Ratner-type dyads and rectification studies in Langmuir–Blodgett (LB) films. *Chem. Eur. J.* 2016, **22**, 10539-10547.
19. Terada, K.-i.; Nakamura, H.; Kanaizuka, K.; Haga, M. a.; Asai, Y.; Ishida, T., Long-Range Electron Transport of Ruthenium-Centered Multilayer Films via a Stepping-Stone Mechanism. *ACS Nano* 2012, **6**, 1988-1999.
 20. Pathak, A.; Bora, A.; Liao, K.-C.; Schmolke, H.; Jung, A.; Klages, C.-P.; Schwartz, J.; Tornow, M., Disorder-Derived, Strong Tunneling Attenuation in Bis-Phosphonate Monolayers. *J. Phys. Condens. Matter* 2016, 094008.
 21. Herrero, I. L.; Ismael, A. K.; Milán, D. C.; Vezzoli, A.; Martín, S.; González-Orive, A.; Grace, I.; Lambert, C.; Serrano, J. L.; Nichols, R. J.; Cea, P., Unconventional Single-Molecule Conductance Behavior for a New Heterocyclic Anchoring Group: Pyrazolyl. *J. Phys. Chem. Lett.* 2018, **9**, 5364-5372.
 22. Herrero, L.; Ismael, A.; Martín, S.; Milan, D. C.; Serrano, J. L.; Nichols, R. J.; Lambert, C.; Cea, P., Single molecule vs. large area design of molecular electronic devices incorporating an efficient 2-aminepyridine double anchoring group. *Nanoscale* 2019, **11**, 15871-15880.
 23. Ye, Q.; Wang, H.; Yu, B.; Zhou, F., Self-assembly of catecholic ferrocene and electrochemical behavior of its monolayer. *RSC Advances* 2015, **5**, 60090-60095.
 24. Wei, Z.; Wang, X.; Borges, A.; Santella, M.; Li, T.; Sørensen, J. K.; Vanin, M.; Hu, W.; Liu, Y.; Ulstrup, J.; Solomon, G. C.; Chi, Q.; Bjørnholm, T.; Nørgaard, K.; Laursen, B. W., Triazatriangulene as Binding Group for Molecular Electronics. *Langmuir* 2014, **30**, 14868-14876.
 25. Kuhn, S.; Jung, U.; Ulrich, S.; Herges, R.; Magnussen, O., Adlayers based on molecular platforms of trioxatriangulenium. *Chem. Com.* 2011, **47**, 8880-8882.
 26. Katano, S.; Kim, Y.; Kitagawa, T.; Kawai, M., Tailoring electronic states of a single molecule using adamantane-based molecular tripods. *Phys. Chem. Chem. Phys.* 2013, **15**, 14229-14233.
 27. Gerhard, L.; Edelmann, K.; Homberg, J.; Valášek, M.; Bahoosh, S. G.; Lukas, M.; Pauly, F.; Mayor, M.; Wulfhekel, W., An electrically actuated molecular toggle switch. *Nat. Commun.* 2017, **8**, 14672.
 28. Ie, Y.; Hirose, T.; Nakamura, H.; Kiguchi, M.; Takagi, N.; Kawai, M.; Aso, Y., Nature of Electron Transport by Pyridine-Based Tripodal Anchors: Potential for Robust and Conductive Single-Molecule Junctions with Gold Electrodes. *J. Am. Chem. Soc.* 2011, **133**, 3014-3022.
 29. Sakamoto, R.; Ohirabaru, Y.; Matsuoka, R.; Maeda, H.; Katagiri, S.; Nishihara, H., Orthogonal bis(terpyridine)–Fe(II) metal complex oligomer wires on a tripodal scaffold: rapid electron transport. *Chem. Com.* 2013, **49**, 7108-7110.
 30. Kiguchi, M.; Takahashi, Y.; Fujii, S.; Takase, M.; Narita, T.; Iyoda, M.; Horikawa, M.; Naitoh, Y.; Nakamura, H., Additive Electron Pathway and Nonadditive Molecular Conductance by Using a Multipodal Bridging Compound. *J. Phys. Chem.* 2014, **118**, 5275-5283.
 31. Sebechlebska, T.; Sebera, J.; Kolivoska, V.; Lindner, M.; Gasiot, J.; Meszaros, G.; Valasek, M.; Mayor, M.; Hromadova, M., Investigation of the geometrical arrangement and single molecule charge transport in self-assembled monolayers of molecular towers based on tetraphenylmethane tripod. *Electrochim. Acta* 2017, **258**, 1191-1200.
 32. O'Driscoll, L. J.; Wang, X.; Jay, M.; Batsanov, A. S.; Sadeghi, H.; Lambert, C. J.; Robinson, B. J.; Bryce, M. R., Carbazole-Based Tetrapodal Anchor Groups for Gold

- Surfaces: Synthesis and Conductance Properties. *Ang. Chem. Int. Ed.* 2020, **59**, 882-889.
33. Li, Z.; Smeu, M.; Afsari, S.; Xing, Y.; Ratner, M. A.; Borguet, E., Single-Molecule Sensing of Environmental pH—an STM Break Junction and NEGF-DFT Approach. *Angewandte Chemie International Edition* 2014, **53**, 1098-1102.
 34. Cai, S.; Deng, W.; Huang, F.; Chen, L.; Tang, C.; He, W.; Long, S.; Li, R.; Tan, Z.; Liu, J.; Shi, J.; Liu, Z.; Xiao, Z.; Zhang, D.; Hong, W., Light-Driven Reversible Intermolecular Proton Transfer at Single-Molecule Junctions. *Ang. Chem. Int. Ed.* 2019, **58**, 3829-3833.
 35. Brooke, R. J.; Szumski, D. S.; Vezzoli, A.; Higgins, S. J.; Nichols, R. J.; Schwarzacher, W., Dual Control of Molecular Conductance through pH and Potential in Single-Molecule Devices. *Nano Letters* 2018, **18**, 1317-1322.
 36. Nishino, T.; Hayashi, N.; Bui, P. T., Direct Measurement of Electron Transfer through a Hydrogen Bond between Single Molecules. *J. Am. Chem. Soc.* 2013, **135**, 4592-4595.
 37. Wu, C.; Alqahtani, A.; Sangtarash, S.; Vezzoli, A.; Sadeghi, H.; Robertson, C. M.; Cai, C.; Lambert, C. J.; Higgins, S. J.; Nichols, R. J., In situ formation of H-bonding imidazole chains in break-junction experiments. *Nanoscale* 2020, **12**, 7914-7920.
 38. Chang, S. C.; He, J.; Lin, L.; Zhang, P.; Liang, F.; Young, M.; Huang, S.; Lindsay, S., Tunnel conductance of Watson-Crick nucleoside-base pairs from telegraph noise. *Nanotechnology* 2009, **20**, 185102.
 39. Zhou, C.; Li, X.; Gong, Z.; Jia, C.; Lin, Y.; Gu, C.; He, G.; Zhong, Y.; Yang, J.; Guo, X., Direct observation of single-molecule hydrogen-bond dynamics with single-bond resolution. *Nat. Commun.* 2018, **9**, 807.
 40. Pan, X.; Lawson, B.; Rustad, A. M.; Kamenetska, M., pH-Activated Single Molecule Conductance and Binding Mechanism of Imidazole on Gold. *Nano Letters* 2020, **20**, 4687-4692.
 41. Ai, Q.; Fu, Q.; Liang, F., pH-Mediated Single Molecule Conductance of Cucurbit[7]uril. *Front. Chem.* 2020, **8**.
 42. Galli, S.; Maspero, A.; Giacobbe, C.; Palmisano, G.; Nardo, L.; Comotti, A.; Bassanetti, I.; Sozzani, P.; Masciocchi, N., When long bis(pyrazolates) meet late transition metals: structure, stability and adsorption of metal-organic frameworks featuring large parallel channels. *J. Mater. Chem. A* 2014, **2**, 12208-12221.
 43. Herrer, L.; Martín, S.; Cea, P., Nanofabrication Techniques in Large Area Molecular Electronic Devices. *Appl. Sci.* 2020, **10**, 6064.
 44. Villares, A.; Lydon, D. P.; Porres, L.; Beeby, A.; Low, P. J.; Cea, P.; Royo, F. M., Preparation of ordered films containing a phenylene ethynylene oligomer by the Langmuir-Blodgett technique. *J. Phys. Chem. B.* 2007, **111**, 7201-7209.
 45. Ballesteros, L. M.; Martín, S.; Momblona, C.; Marqués-González, S.; López, M. C.; Nichols, R. J.; Low, P. J.; Cea, P., Acetylene used as a new linker for molecular junctions in phenylene-ethynylene oligomer Langmuir-Blodgett films. *J. Phys. Chem. C.* 2012, **116**, 9142-9150.
 46. Ballesteros, L. M.; Martín, S.; Marqués-González, S.; López, M. C.; Higgins, S.; Nichols, R. J.; Low, P. J.; Cea, P., Single gold atom containing oligo(phenylene)ethynylene: assembly into LB films and electrical characterization. *J. Phys. Chem. C.* 2015, **119**, 784-773.
 47. Villares, A.; Pera, G.; Martín, S.; Nichols, R. J.; Lydon, D. P.; Applegarth, L.; Beeby, A.; Low, P. J.; Cea, P., Fabrication, Characterization, and Electrical Properties of Langmuir-Blodgett Films of an Acid Terminated Phenylene-Ethynylene Oligomer. *Chem. Mater.* 2010, **22**, 2041-2049.

48. Osorio, H. M.; Martín, S.; Carmen Lopez, M.; Marques-Gonzalez, S.; Higgins, S. J.; Nichols, R. J.; Low, P. J.; Cea, P., Electrical characterization of single molecule and Langmuir-Blodgett monomolecular films of a pyridine-terminated oligo(phenylene-ethynylene) derivative. *Beilstein J. Nanotechnol.* 2015, **6**, 1145-1157.
49. Ballesteros, L. M.; Martín, S.; Pera, G.; Schauer, P. A.; Kay, N. J.; López, M. C.; Low, P. J.; Nichols, R. J.; Cea, P., Directionally oriented LB films of an OPE derivative: assembly, characterization, and electrical properties *Langmuir* 2011, **27**, 3600-3610.
50. Haiss, W.; Wang, C.; Grace, I.; Batsanov, A. S.; Schiffrin, D. J.; Higgins, S. J.; Bryce, M. R.; Lambert, C. J.; Nichols, R. J., Precision control of single-molecule electrical junctions. *Nat. Mater.* 2006, **5**, 995-1002.
51. Diez-Perez, I.; Hihath, J.; Hines, T.; Wang, Z.-S.; Zhou, G.; Müllen, K.; Tao, N., Controlling single-molecule conductance through lateral coupling of π orbitals. *Nat. Nanotechnology* 2011, **6**, 226-231.
52. Johnson, C. R.; Henderson, W. W.; Shepherd, R. E., Pyrazole imidazole and pyrazolato imidazolato complexes of pentacyanoferrate(II-III) and pentaammineruthenium (II-III) - LMCT transitions of low-spin D5 complexes *Inorg. Chem.* 1984, **23**, 2754-2763.
53. Lee, H.; Berezin, M. Y.; Tang, R.; Zhegalova, N.; Achilefu, S., Pyrazole-substituted Near-infrared Cyanine Dyes Exhibit pH-dependent Fluorescence Lifetime Properties. *Photochem. Photobiol.* 2013, **89**, 326-331.
54. Wassermann, T. N.; Rice, C. A.; Suhm, M. A.; Luckhaus, D., Hydrogen bonding lights up overtones in pyrazoles. *J. Chem. Phys.* 2007, **127**, 234309.
55. Su, P.; Song, X.-G.; Sun, R.-Q.; Xu, X.-M., Hydrogen bonding in the crystal structure of the molecular salt of pyrazole-pyrazolium picrate. *Acta Crystallogr. E Crystallogr. Commun.* 2016, **72**, 861-863.
56. Bertolasi, V.; Gilli, P.; Ferretti, V.; Gilli, G.; Fernández-Castaño, C., Self-assembly of N H-pyrazoles via intermolecular N-H ... N hydrogen bonds. *Acta Crystallogr. Section B* 2000, **55**, 985-993.
57. Pera, G.; Martín, S.; Ballesteros, L. M.; Hope, A. J.; Low, P. J.; Nichols, R. J.; Cea, P., Metal-Molecule-Metal Junctions in Langmuir-Blodgett Films Using a New Linker: Trimethylsilane. *Chem. Eur. J.* 2010, **16**, 13398-13405.